NIH Public Access
Author Manuscript
Mol Cell Neurosci. Author manuscript; available in PMC 2014 May 01.

Published in final edited form as:
Mol Cell Neurosci. 2013 May ; 54: 22–29. doi:10.1016/j.mcn.2012.12.005.

Human immunodeficiency virus-1 protein Tat induces excitotoxic loss of presynaptic terminals in hippocampal cultures

Angela H. Shin[a] and **Stanley A. Thayer**[a,b]

Angela H. Shin: shinx068@umn.edu; Stanley A. Thayer: sathayer@umn.edu

[a]Department of Pharmacology, University of Minnesota Medical School, Minneapolis, MN 55455 USA

Abstract

Human Immunodeficiency Virus (HIV) infection of the CNS produces dendritic damage that correlates with cognitive decline in patients with HIV-associated neurocognitive disorders (HAND). HIV-induced neurotoxicity results in part from viral proteins shed from infected cells, including the HIV transactivator of transcription (Tat). We previously showed that Tat binds to the low density lipoprotein receptor-related protein (LRP), resulting in overactivation of NMDA receptors, activation of the ubiquitin-proteasome pathway, and subsequent loss of postsynaptic densities. Here, we show that Tat also induces a loss of presynaptic terminals. The number of presynaptic terminals was quantified using confocal imaging of synaptophysin fused to green fluorescent protein (Syn-GFP). Tat-induced loss of presynaptic terminals was secondary to excitatory postsynaptic mechanisms because treatment with an LRP antagonist or an NMDA receptor antagonist inhibited this loss. Treatment with nutlin-3, an E3 ligase inhibitor, prevented Tat-induced loss of presynaptic terminals. These data suggest that Tat-induced loss of presynaptic terminals is a consequence of excitotoxic postsynaptic activity. We previously found that ifenprodil, an NR2B subunit-selective NMDA receptor antagonist, induced recovery of postsynaptic densities. Here we show that Tat-induced loss of presynaptic terminals was reversed by ifenprodil treatment. Thus, Tat-induced loss of presynaptic terminals is reversible, and this recovery can be initiated by inhibiting a subset of postsynaptic NMDA receptors. Understanding the dynamics of synaptic changes in response to HIV infection of the CNS may lead to the design of improved pharmacotherapies for HAND patients.

Keywords

presynaptic terminal; HIV-1 Tat; synapse loss; HIV-associated neurocognitive disorders; excitotoxicity

© 2012 Elsevier Inc. All rights reserved.

[b]Corresponding author: Stanley A. Thayer, Department of Pharmacology, University of Minnesota, 6-120 Jackson Hall, 321 Church Street SE, Minneapolis, MN 55455, USA Tel.: +1-612-626-7049; Fax: +1-612-625-8408; sathayer@umn.edu.

Publisher's Disclaimer: This is a PDF file of an unedited manuscript that has been accepted for publication. As a service to our customers we are providing this early version of the manuscript. The manuscript will undergo copyediting, typesetting, and review of the resulting proof before it is published in its final citable form. Please note that during the production process errors may be discovered which could affect the content, and all legal disclaimers that apply to the journal pertain.

NIH-PA Author Manuscript
NIH-PA Author Manuscript
NIH-PA Author Manuscript

NIH-PA Author Manuscript
NIH-PA Author Manuscript
NIH-PA Author Manuscript

Introduction

Human immunodeficiency virus (HIV) infection is a worldwide epidemic that affects approximately 30 million people (Kaul et al., 2001). Neurocognitive deficits are a significant consequence of HIV infection and affect approximately 30–50% of HIV-infected patients (Cysique et al., 2004; Tozzi et al., 2005). Neurological symptoms range in severity from mild cognitive impairment to severe HIV-associated dementia, and are collectively known as HIV-associated neurocognitive disorders (HAND) (Ellis et al., 2007). HAND is a major consequence of HIV infection; progression of these neurological symptoms often renders patients incapable of functioning without daily assistance (Hult et al., 2008; Kaul and Lipton, 2006; Minagar et al., 2008). Additionally, while the advent of combined anti-retroviral therapies has reduced the incidence of HIV-associated dementia, the increased lifespan of HIV-infected patients has increased the prevalence of HAND diagnoses, providing a compelling need to develop improved therapies to combat the rising incidence of HAND.

HIV induces neurotoxicity and subsequent neurocognitive deficits by an indirect mechanism. The virus infects macrophages and microglia, not neurons in the CNS, and these infected cells in turn secrete inflammatory cytokines and shed viral proteins that are toxic to neurons (Genis et al., 1992; Speth et al., 2001). One such toxic protein is the HIV Transactivator of transcription (Tat), which is shed by infected cells. Tat mRNA and protein are found in the CNS of HAND patients (Del Valle et al., 2000; Hofman et al., 1994; Hudson et al., 2000; Wiley et al., 1996) and Tat protein induces HAND neuropathologies in vivo (Fitting et al., 2010; Kim et al., 2003). In vitro effects of Tat include dendritic pruning, decreased spine density, and synapse loss (Eugenin et al., 2007; Kim et al., 2008; Liu et al., 2000). Clinical studies have shown that the extent of cognitive decline in HAND patients correlates closely with dendritic damage and synapse loss, rather than overt neuronal death (Sa et al., 2004; Wiley et al., 1999).

Tat induces the loss of excitatory synapses via a mechanism that is distinct from that by which it elicits cell death (Kim et al., 2008). Tat binds to the low density lipoprotein receptor-related protein (LRP), and activates NMDA receptors. The subsequent postsynaptic calcium influx triggers two independent pathways. Loss of the postsynaptic density results from calcium-induced activation of an ubiquitin ligase. Cell death results from calcium-dependent activation of neuronal nitric oxide synthase (nNOS) (Kim et al., 2008). Interestingly, Tat-induced loss of postsynaptic densities is reversible. What is not known, however, is how loss and recovery of postsynaptic densities relates to the dynamics of presynaptic terminals during exposure to HIV-1 Tat.

Synaptophysin is an abundant membrane glycoprotein found on synaptic vesicles at the presynaptic terminal (Johnston and Sudhof, 1990; Rehm et al., 1986; Wiedenmann and Franke, 1985). Synaptophysin is a calcium-binding protein that is nonessential for vesicle release (McMahon et al., 1996), and is a major component of small synaptic vesicles. It is recruited to presynaptic active zones during synaptogenesis, albeit later than precursor proteins such as Bassoon or Piccolo (Fletcher et al., 1991; Friedman et al., 2000; Ziv and Garner, 2004), and is thus a good marker for presynaptic terminals.

In this study, we examined the effects of HIV-1 Tat on presynaptic terminals by tracking the expression of a synaptophysin-GFP fusion protein. HIV-1 Tat decreased the number of presynaptic terminals on hippocampal neurons in culture. Moreover, this loss was triggered by NMDA receptor activity, indicating that loss of presynaptic terminals was initiated by postsynaptic mechanisms. Tat-induced loss of presynaptic terminals was reversible, and this

NIH-PA Author Manuscript

NIH-PA Author Manuscript

NIH-PA Author Manuscript

recovery was initiated by modulating NMDA receptor activity. These results suggest that Tat-induced synapse loss and recovery are driven by postsynaptic mechanisms.

Material and methods

Materials

Materials were obtained from the following sources: the Syn-GFP expression vector (pSynaptophysin-GFP-C1) was kindly provided by Jane Sullivan (University of Washington, Seattle, WA); the expression vector for DsRed2 (pDsRed2-N1) from Clontech (Mountain View, CA); HIV-1 Tat (Clade B, full length, recombinant) from Prospec Tany TechnoGene Ltd. (Rehovot, Israel) and through the NIH AIDS Research and Reference Reagent Program (HIV-1 Tat protein (full length, Clade B) from Dr. John Brady and DAIDS, NIAID); recombinant rat receptor associated protein (RAP) from Fitzgerald Industries International (Concord, MA); Dulbecco's modified Eagle medium (DMEM), fetal bovine serum, and horse serum from Invitrogen (Carlsbad, CA); ifenprodil hemitartrate from Tocris (Ellsville, MO); penicillin/streptomycin, MK801, and all other reagents from Sigma (St. Louis, MO). For control experiments, Tat was heat-inactivated by incubation at 85°C for 30 min.

Cell culture

Rat hippocampal neurons were grown in primary culture as described previously (Shen and Thayer, 1998). Fetuses were removed on embryonic day 17 from maternal rats euthanized by CO_2 inhalation. Hippocampi were dissected and placed in Ca^{2+} and Mg^{2+}-free HEPES-buffered Hanks salt solution (HHSS), pH 7.45. HHSS was composed of the following (in mM): HEPES 20, NaCl 137, $CaCl_2$ 1.3, $MgSO_4$ 0.4, $MgCl_2$ 0.5, KCl 5.0, KH_2PO_4 0.4, Na_2HPO_4 0.6, $NaHCO_3$ 3.0, and glucose 5.6. Cells were dissociated by trituration through a 5 ml pipette and a flame-narrowed Pasteur pipette and resuspended in DMEM without glutamine, supplemented with 10% fetal bovine serum and penicillin/streptomycin (100 U/ml and 100 μg/ml, respectively). Dissociated cells were then plated at a density of 100,000–120,000 cells per dish onto a 25-mm-round cover glass (#1) glued to cover a 19 mm diameter opening drilled through the bottom of a 35 mm Petri dish. The cover glass was precoated with Matrigel (200 μL, 0.2mg/mL) (BD Biosciences, Billerica, MA). Neurons were grown in a humidified atmosphere of 10% CO_2 and 90% air (pH 7.4) at 37 °C, and fed on days 1 and 6 by exchange of 75% of the media with DMEM, supplemented with 10% horse serum and penicillin/streptomycin. Cells used in these experiments were cultured without mitotic inhibitors for at least 12 days, resulting in a mixed glial-neuronal culture. Immunocytochemistry experiments demonstrated that these cultures were composed of 18 2 % neurons, 70 3 % astrocytes and 9 3 % microglia (Kim et al., 2011).

Transfection

Rat hippocampal neurons were transfected between 10 and 12 days in vitro using a modification of a protocol described previously (Kim et al., 2008). Briefly, hippocampal cultures were incubated for at least 20 minutes in DMEM supplemented with 1 mM kynurenic acid, 10 mM $MgCl_2$, and 5 mM HEPES, to reduce neurotoxicity. A DNA/calcium phosphate precipitate containing 1 μg total plasmid DNA per well was prepared, allowed to form for 30 min at room temperature, and added to the culture. After a 90 minute incubation period, cells were washed once with DMEM supplemented with $MgCl_2$ and HEPES and then returned to conditioned media, saved at the beginning of the procedure. Transfected neurons were imaged 48–72 hours post-transfection. Transfection efficiency ranged from 1–5%.

NIH-PA Author Manuscript

NIH-PA Author Manuscript

NIH-PA Author Manuscript

Confocal imaging

Petri dishes containing transfected neurons were sealed with Parafilm, transferred to the stage of an inverted confocal microscope (Olympus Fluoview 300, Melville, NY) and viewed through a 60X oil-immersion objective (NA=1.4). To enable repeated imaging of the same cell over a 24 h period, the location of the cell was recorded using micrometers attached to the stage of the microscope. Optical sections spanning 8 μm in the z-dimension were collected (1 μm steps), and were combined through the z-axis into a compressed z stack. GFP was excited at 488 nm with an argon ion laser and emission collected at 530 nm (10 nm band pass). DsRed2 was excited at 543 nm with a green HeNe laser and emission collected at >605 nm. The cell culture dish was returned to the CO_2 incubator between image collections. Experiments studying synapse recovery were performed for 24 hours in the continuous presence of Tat, with or without the specified drugs added at 16 hours.

Image processing

To count and label Syn-GFP puncta an automated algorithm was created using MetaMorph 6.2 image processing software described previously (Waataja et al., 2008). Briefly, maximum z-projection images were created from the DsRed2 and GFP image stacks. Next, a threshold set 1 s.d. above the image mean was applied to the DsRed2 image. This created a 1-bit image that was used as a mask via a logical AND function with the GFP maximum z-projection. A top-hat filter (80 pixels) was applied to the masked Syn-GFP image. A threshold set 1.5 s.d. above the mean intensity inside the mask was then applied to the contrast enhanced image. Structures between 8 and 80 pixels (approximately 0.66 to 6.64 μm in diameter) and in contact with the DsRed2 mask were counted as presynaptic terminals. The structures were then dilated and superimposed on the DsRed2 maximum z-projection for visualization. All Syn-GFP puncta in the representative processed images displayed in the figures were included in the quantitative analysis.

Immunocytochemistry

Hippocampal cultures were prepared as described above and maintained for at least 12 days in culture. Cells on coverslips were transfected with an expression plasmid for Syn-GFP as described above. After 48 hrs, cells were washed with tris-buffered saline (TBS), and then fixed with Lana's fixative (8% paraformaldehyde, 14% picrate, 0.16 M PO_4) for 10 min. The cells were washed with TBS, then permeablized in TBS + 0.2% Triton X100 (Sigma) for 10 min at room temperature. After permeablization, cells were incubated with mouse anti-Bassoon monoclonal antibody (1:200, Enzo Life Sciences, Farmingdale, NY) in TBS + 0.2% Tween-20 (Sigma) for 1 h at room temperature. Cells were washed with TBS and labeled with tetramethyl rhodamine isothiocyanate (TRITC)-conjugated goat anti-mouse antibody (Millipore, Billerica, MA, 1:400) in TBS + 0.2% Tween-20. Coverslips were mounted with DPX mountant (Sigma) and visualized on an inverted confocal microscope (Olympus Fluoview 300, Melville, NY) using a 60X oil-immersion objective (NA=1.4). TRITC was excited at 543 nm, and emission collected at >605 nm.

Statistics

For synapse loss and recovery studies, an individual experiment (n=1) was defined as the change in the number of Syn-GFP puncta from a single cell from a single coverslip. Puncta counts were presented as mean ± SEM. Each experiment was replicated over at least 3 separate cultures. In all statistical analyses we used Student's t-test for single or ANOVA with Tukey's post-hoc test for multiple statistical comparisons (OriginPro v8.5, Northampton, MA).

NIH-PA Author Manuscript

NIH-PA Author Manuscript

NIH-PA Author Manuscript

Results

Synaptophysin-GFP labels presynaptic terminals

The number of presynaptic terminals in rat hippocampal cultures was measured by confocal imaging of neurons transfected with an expression construct for the presynaptic protein synaptophysin fused to GFP (Syn-GFP). Synaptophysin is part of the neurotransmitter release machinery and is an established marker for presynaptic terminals. The neurons were co-transfected with an expression construct for DsRed2, a red fluorescent protein that filled the neuron and enabled visualization of cell morphology (Fig. 1A, DsRed). Syn-GFP expressed in a distinct punctate pattern (Fig. 1A, Syn-GFP). Neurons were imaged on a laser scanning confocal microscope as described in Methods. Image processing identifed Syn-GFP puncta meeting size and intensity criteria in contact with DsRed2 fluorescence, using a previously described algorithm (Shin et al., 2012). These puncta were dilated and overlaid on the DsRed2 maximum projection for visualization purposes (Fig. 1A, Processed). The same neuron was repeatedly imaged over time and the number of Syn-GFP puncta counted at each time point to determine changes in number of presynaptic terminals impinging on a single cell.

Syn-GFP puncta represented presynaptic terminals because they co-localized with Bassoon immunoreactivity (Fig. 1B). Bassoon is a scaffolding protein concentrated at presynaptic terminals (tom Dieck et al., 1998). 78 ± 4% of Syn-GFP puncta co-localized with Bassoon immunoreactivity, confirming that Syn-GFP expression in our culture accurately labels presynaptic terminals. The presynaptic terminals seen are a mixture of autapses resulting from an axon extending from the DsRed filled soma displayed in the field as well as boutons from axons emanating from cells outside the field of view.

HIV-1 Tat induces loss of Syn-GFP puncta

We previously found that 24 hr exposure to the HIV-1 Tat protein decreased the number of postsynaptic densities in hippocampal neurons in culture (Kim et al., 2008). Here, we studied the effects of Tat on presynaptic terminals. As shown in Figure 2A, 24 hr treatment with Tat produced a marked decrease in the number of Syn-GFP puncta. Treatments of this duration did not produce cell death (Kim et al., 2008), nor did Tat significantly alter cell morphology (Fig. 2A). Figure 2B shows the time course for changes in the number of Syn-GFP puncta during exposure to 50 ng/mL Tat. HIV-1 Tat induced an 8 ± 4% loss in the number of Syn-GFP puncta by 8 h, 8 ± 4% loss by 16 h, and 13 ± 4% loss by 24 h. This loss was significant relative to control values by 16 h, and sustained over a 48 h interval. This time course is similar to that seen for Tat-induced changes in postsynaptic densities (Kim et al., 2008). In contrast to Tat-treated cells, control cells exhibited a 25 ± 12% increase in the number of Syn-GFP puncta over 48 h. Heat-inactivated Tat did not induce a loss in the number of Syn-GFP puncta (26 ± 8% increase, n = 6), confirming that Syn-GFP loss was due to functional HIV-1 Tat protein.

Tat-induced Syn-GFP loss is dependent on postsynaptic activity

Loss of postsynaptic densities is initiated by Tat binding to the low density lipoprotein receptor-related protein (LRP), and over-activating NMDA receptors. We sought to determine whether the same mechanisms were involved in Tat-induced Syn-GFP loss. Tat (50 ng/mL) induced a 15 3 % loss of Syn-GFP puncta (Fig. 3A). Pre-treating neurons with the LRP antagonist receptor-associated protein (RAP, 50 nM) prior to Tat exposure, inhibited Tat-induced Syn-GFP loss (Fig. 3, A–B). Additionally, pre-treating neurons with the NMDA receptor antagonist MK801 (10 μM) prior to Tat exposure inhibited Tat-induced Syn-GFP loss. We previously showed that both RAP and MK801 inhibited Tat-induced loss

NIH-PA Author Manuscript

NIH-PA Author Manuscript

NIH-PA Author Manuscript

of post-synaptic densities (Kim et al., 2008). These data are consistent with the idea that loss of presynaptic terminals induced by Tat is driven by its activity on postsynaptic sites.

Tat-induced loss of postsynaptic densities required ubiquitination of PSD95 and proteasomal degradation; inhibition of the E3 ligase MDM2 with the antagonist nutlin-3 prevented Tat-induced loss of postsynaptic densities (Kim et al., 2008). Pretreating neurons with 1 μM nutlin-3 prior to Tat exposure inhibited Tat-induced Syn-GFP loss (Fig. 4, A–B). These data indicate that ubiquitination of postsynaptic proteins is required for loss of presynaptic terminals during Tat exposure.

Tat-induced Syn-GFP loss is reversible

Tat-induced loss of postsynaptic densities is reversible (Kim et al., 2008). Treating neurons with ifenprodil, an NR2B subunit-selective NMDA receptor antagonist, during Tat exposure induced recovery of postsynaptic densities, whereas no spontaneous recovery was seen in the absence of drug (Shin et al., 2012). We sought to determine whether presynaptic terminals could also be recovered after Tat-induced loss. Neurons were treated with 50 ng/mL Tat for 16 hrs, and then treated with 10 μM ifenprodil. Application of ifenprodil induced a recovery in the number of Syn-GFP puncta, whereas no recovery was seen without ifenprodil treatment (Fig. 5, A–B). These data indicate that Tat-induced loss of presynaptic terminals is reversible. Furthermore, because ifenprodil acts on postsynaptic NMDA receptors, this recovery was initiated by altered postsynaptic activity.

Discussion

Dendritic pruning and synapse loss are hallmarks of HAND pathology (Everall et al., 1999; Masliah et al., 1997). The HIV-1 protein Tat is shed by infected cells in the central nervous system and *in vitro*, it binds LRP to activate NMDA receptors, resulting in the loss of postsynaptic densities (Kim et al., 2008; Shin et al., 2012). Here, we examined the effects of Tat on presynaptic terminals. Tat induced loss of presynaptic terminals that mirrored loss of postsynaptic densities with respect to time course and pharmacology. Loss of presynaptic terminals was dependent on postsynaptic activity, suggesting that Tat acts directly on the postsynaptic density, and that loss of presynaptic terminals is a consequence of this action. Tat-induced loss of presynaptic terminals was reversible, and recovery of the number of presynaptic terminals was evoked by inhibition of NR2B-containing NMDA receptors. Thus, the mechanism of recovery of presynaptic terminals after Tat-induced loss is also dependent upon postsynaptic activity.

We imaged Syn-GFP to visualize presynaptic terminals on individual neurons. Syn-GFP expressed as distinct puncta that co-localized with immunoreactivity for the presynaptic marker protein Bassoon, indicating that Syn-GFP fluorescence was appropriately localized to presynaptic terminals. Furthermore, we have previously shown that Syn-GFP puncta responded to other stimuli such as IL-1β or lithium, treatments that induce decreases and increases in the number of postsynaptic densities, respectively (Kim and Thayer, 2009; Mishra et al., 2012). Therefore, Syn-GFP is a valid and responsive marker for presynaptic terminals and suitable for live cell imaging.

Tat mRNA was detected in brain extracts from patients with HIV encephalitis but not in samples from HIV patients without dementia (Hudson et al., 2000). Tat protein levels in the serum of HIV patients are in the low ng/mL range (Westendorp et al., 1995; Xiao et al., 2000). The Tat protein detected in the brains of patients with HIV encephalitis using immunohistochemistry indicated that Tat was taken up by cells (Del Valle et al., 2000), consistent with the LRP mediated mechanism that underlies the synapse loss we describe in vitro. Soluble Tat has not been measured in the CNS of HAND patients, an observation

NIH-PA Author Manuscript

NIH-PA Author Manuscript

NIH-PA Author Manuscript

thought to result from LRP-mediated uptake in vivo and rapid proteolysis in post mortem tissue (Li et al., 2009). Previous work from our lab found the EC_{50} for Tat in this assay to be approximately 6 ng/mL, which is well within the concentration range used in vitro (Aksenova et al., 2008; Eugenin et al., 2007; Li et al., 2008). We used a maximally effective concentration of Tat (50 ng/mL) in the present study.

HIV-1 Tat induced a 15 ± 3% decrease in the number of Syn-GFP puncta over 24 hours. RAP, an LRP antagonist, and MK801, an NMDA receptor antagonist, both inhibited Tat-induced loss of Syn-GFP puncta, indicating that Tat binding to LRP and subsequent activation of NMDA receptors were required for Tat-induced loss of presynaptic terminals. NMDA receptor activation and subsequent loss of presynaptic terminals are also seen in other neurotoxic processes. For example, treatment with the inflammatory cytokine IL-1β induced loss of Syn-GFP puncta that was also prevented by MK801 (Mishra et al., 2012). LRP and NMDA receptors are highly expressed at postsynaptic densities and Tat forms a macromolecular complex with LRP, the NMDA receptor and PSD95 (Eugenin et al., 2007). Tat has been shown to alter the expression and activity of presynaptic neurotransmitter transporters in other brain regions, such as the dopamine transporter in the striatum and midbrain (Midde et al., 2012; Perry et al., 2010) and the vesicular monoamine transporter-2 in the striatum (Theodore et al., 2012). However, there is no evidence suggesting that Tat binds to presynaptic targets or exerts any direct presynaptic effects in the hippocampus. Thus, we suggest that Tat-induced synapse loss described here is initiated by postsynaptic processes. However, the temporal resolution of our experiments could not resolve a clear chronological sequence for the loss of the PSD versus the presynaptic terminal. In summary, Tat clearly initiates the loss of both pre- and post-synaptic structures by binding to postsynaptic LRP but, we did not determine whether the PSD or presynaptic terminal was lost first.

Treatment with nutlin-3, an inhibitor of the E3 ligase MDM2, prevented Tat-induced loss of presynaptic terminals. MDM2 ubiquitinates PSD95 (Bianchetta et al., 2011; Colledge et al., 2003), but no evidence suggests MDM2-mediated ubiquitination of presynaptic proteins, suggesting that postsynaptic E3 ligase activity was required for loss of Syn-GFP puncta. Treatment with nutlin-3 prevents Tat-induced degradation of PSD95 (Kim et al., 2008), consistent with the idea that inhibition of MDM2 prevents degradation of postsynaptic proteins that are required for synapse maturation and maintenance. Other than PSD95, we have not identified specific postsynaptic proteins responsible for the presynaptic loss described here. However, there is precedent for postsynaptic proteins coordinating presynaptic stability by direct interactions such as those mediated by cadherins, integrins, and neuroligin (Chavis and Westbrook, 2001; Scheiffele et al., 2000; Togashi et al., 2002). It is possible that postsynaptic proteins are ubiquitinated concurrently with PSD95 in the presence of Tat, alternatively, loss of PSD95 might affect the function of proteins that interact with it (Meyer et al., 2004). The mechanism by which synaptophysin is eliminated from the presynaptic terminal has yet to be elucidated; our assay cannot distinguish diffusion of Syn-GFP out of the presynaptic terminal from degradation.

Finding that Tat-induced loss of presynaptic terminals was reversible is particularly interesting. We had previously shown that Tat-induced loss of postsynaptic densities could be reversed by ifenprodil, an antagonist for NR2B-containing NMDA receptors. In the current study we show that ifenprodil induced recovery of presynaptic terminals as well. No spontaneous recovery was seen; Tat-induced loss of presynaptic terminals was only reversed in the presence of ifenprodil. This observation further supports our contention that the postsynaptic side of the synapse drives loss and recovery. These data indicate that the NR2B-containing NMDA receptors inhibit recovery of synapses after Tat exposure. The mechanism by which NR2B-containing NMDA receptors regulate synapse recovery is

NIH-PA Author Manuscript

NIH-PA Author Manuscript

NIH-PA Author Manuscript

unclear. Immunocytochemistry experiments indicate that the hippocampal cultures used here express both NR2A-containing and NR2B-containing NMDA receptors (Shin et al., 2012). Many studies have shown that NR2A versus NR2B-containing NMDA receptors have distinct roles in maintaining neuronal survival, and couple to different downstream effectors (Christopherson et al., 1999; Liu et al., 2004; Liu et al., 2007). NR2A and NR2B-containing NMDA receptors differentially affect Tat-induced postsynaptic changes and neuronal death induced by Tat (Shin et al., 2012). Furthermore, NMDA receptor activity has been shown to inhibit maturation of nascent synapses during synaptogenesis (Gray et al., 2011), and the pathway by which this inhibition occurred is distinct for NR2A-containing receptors versus NR2B-containing receptors. In contrast, inhibition of NR2B-containing NMDA receptors at mature synapses seemed to have little effect. This is consistent with our previous study, which showed that inhibiting NR2B-containing NMDA receptors failed to prevent Tat-induced loss of synapses, but did induce recovery of synapses after the initial loss (Shin et al., 2012).

Tat-induced loss of presynaptic terminals was moderate (−15% change over 24 h), in contrast to the effect seen with the same concentration of Tat at postsynaptic densities (−24% change over 24 h, (Shin et al., 2012)). One possible explanation for this observation is that synaptophysin is expressed at excitatory as well as inhibitory presynaptic terminals (Fykse et al., 1993). Even though the majority of synapses in the hippocampus are glutamatergic, the more moderate effect seen on Syn-GFP puncta may result from an increase in the number of inhibitory synapses as a compensatory measure in response to increased excitation. Indeed, preliminary results from our laboratory indicate that inhibitory synapses increase in number after exposure to HIV-1 Tat (Hargus and Thayer, unpublished observations).

Our results indicate that NR2B-containing receptors play a pivotal role in recovery of presynaptic terminals, and that inhibition of postsynaptic NR2B-containing NMDA receptors is required to initiate synapse recovery after an excitotoxic insult such as HIV-1 Tat. Postsynaptic initiation of the recovery of presynaptic terminals is in contrast to studies observing synaptogenesis, wherein presynaptic molecule recruitment and differentiation precedes postsynaptic development (Friedman et al., 2000; Ziv, 2001). Direct study of the chronology of synapse loss and recovery is limited by the resolution of our assay. However, the pharmacology of presynaptic loss and recovery strongly suggests that postsynaptic signaling initiates both synapse loss and synapse recovery. Therefore, synapse recovery may occur via a novel pathway that requires block of NR2B-containing NMDA receptor activity. Further work is required to eludicate the mechanisms of synapse recovery after Tat-induced loss, and the pathway by which NR2B containing receptors can inhibit recovery.

Conclusions

In conclusion, our study has shown that HIV-1 Tat exposure can induce a reversible loss of presynaptic terminals in hippocampal neurons in culture. This loss and recovery mirrors the effects of Tat on postsynaptic densities and was inhibited by pharmacological agents that act on postsynaptic targets. Thus, the mechanisms initiating both processes are located postsynaptically, in contrast to the mechanisms of synaptogenesis. Eludicating the pathways by which Tat affects the loss and recovery of hippocampal synapses may be crucial to developing targeted therapies for treating HAND. Moreover, the role of NMDA receptor subtypes is crucial to these processes. Common pathways may underlie the synapse loss and recovery associated with many neurodegenerative processes. Determining the signaling pathways activated by NMDA receptor subtypes and how they regulate the loss and recovery of synapses may advance the development of therapeutic approaches to treating neurological disorders of multiple etiologies.

NIH-PA Author Manuscript

NIH-PA Author Manuscript

NIH-PA Author Manuscript

Acknowledgments

The authors would like to thank the NIH AIDS Research and Reference Reagent Program for providing HIV-1 Tat protein, and Dr. Jane Sullivan (University of Washington, Seattle, WA) for providing the synaptophysin-GFP expression construct. The National Institute on Drug Abuse grant DA 07304 supported this work. National Institute on Drug Abuse Training Grant (DA 07234) supported AS.

Abbreviations

HAND	HIV-associated neurocognitive disorders
LRP	Low density lipoprotein receptor-related protein
Tat	Transactivator of transcription
HIV-1	Human immunodeficiency virus-1
Syn	Synaptophysin
DMEM	Dulbecco's modified Eagles media
RAP	receptor associated protein
GFP	green fluorescent protein

References

Aksenova MV, Aksenov MY, Adams SM, Mactutus CF, Booze RM. Neuronal survival and resistance to HIV-1 Tat toxicity in the primary culture of rat fetal neurons. Exp Neurol. 2008; 215:253–263. [PubMed: 19013459]

Bianchetta MJ, Lam TT, Jones SN, Morabito MA. Cyclin-Dependent Kinase 5 Regulates PSD-95 Ubiquitination in Neurons. The Journal of Neuroscience. 2011; 31:12029–12035. [PubMed: 21849563]

Chavis P, Westbrook G. Integrins mediate functional pre- and postsynaptic maturation at a hippocampal synapse. Nature. 2001; 411:317–321. [PubMed: 11357135]

Christopherson KS, Hillier BJ, Lim WA, Bredt DS. PSD-95 Assembles a Ternary Complex with the N-Methyl-D-aspartic Acid Receptor and a Bivalent Neuronal NO Synthase PDZ Domain. J Biol Chem. 1999; 274:27467–27473. [PubMed: 10488080]

Colledge M, Snyder EM, Crozier RA, Soderling JA, Jin Y, Langeberg LK, Lu H, Bear MF, Scott JD. Ubiquitination regulates PSD-95 degradation and AMPA receptor surface expression. Neuron. 2003; 40:595–607. [PubMed: 14642282]

Cysique LA, Maruff P, Brew BJ. Prevalence and pattern of neuropsychological impairment in human immunodeficiency virus–infected/acquired immunodeficiency syndrome (HIV/AIDS) patients across pre- and post-highly active antiretroviral therapy eras: A combined study of two cohorts. J Neurovirol. 2004; 10:350–357. [PubMed: 15765806]

Del Valle L, Croul S, Morgello S, Amini S, Rappaport J, Khalili K. Detection of HIV-1 Tat and JCV capsid protein, VP1, in AIDS brain with progressive multifocal leukoencephalopathy. J Neurovirol. 2000; 6:221–228. [PubMed: 10878711]

Ellis R, Langford D, Masliah E. HIV and antiretroviral therapy in the brain: neuronal injury and repair. Nat Rev Neurosci. 2007; 8:33–44. [PubMed: 17180161]

Eugenin EA, King JE, Nath A, Calderon TM, Zukin RS, Bennett MV, Berman JW. HIV-tat induces formation of an LRP-PSD-95- NMDAR-nNOS complex that promotes apoptosis in neurons and astrocytes. Proc Natl Acad Sci U S A. 2007; 104:3438–3443. [PubMed: 17360663]

Everall IP, Heaton RK, Marcotte TD, Ellis RJ, McCutchan JA, Atkinson JH, Grant I, Mallory M, Masliah E. Cortical synaptic density is reduced in mild to moderate human immunodeficiency virus neurocognitive disorder. HNRC Group. HIV Neurobehavioral Research Center. Brain Pathol. 1999; 9:209–217. [PubMed: 10219738]

NIH-PA Author Manuscript

NIH-PA Author Manuscript

NIH-PA Author Manuscript

Fitting S, Xu R, Bull C, Buch S, El-Hage N, Nath A, Knapp PE, Hauser KF. Interactive Comorbidity between Opioid Drug Abuse and HIV-1 Tat: Chronic Exposure Augments Spine Loss and Sublethal Dendritic Pathology in Striatal Neurons. Am J Pathol. 2010; 177:1397–1410. [PubMed: 20651230]

Fletcher TL, Cameron P, De Camilli P, Banker G. The distribution of synapsin I and synaptophysin in hippocampal neurons developing in culture. The Journal of Neuroscience. 1991; 11:1617–1626. [PubMed: 1904480]

Friedman HV, Bresler T, Garner CC, Ziv NE. Assembly of new individual excitatory synapses: time course and temporal order of synaptic molecule recruitment. Neuron. 2000; 27:57–69. [PubMed: 10939331]

Fykse EM, Takei K, Walch-Solimena C, Geppert M, Jahn R, De Camilli P, Sudhof TC. Relative properties and localizations of synaptic vesicle protein isoforms: the case of the synaptophysins. The Journal of Neuroscience. 1993; 11:4997–5007. [PubMed: 8229211]

Genis P, Jett M, Bernton EW, Boyle T, Gelbard HA, Dzenko K, Keane RW, Resnick L, Mizrachi Y, Volsky DJ, Epstein LG, Gendelman HE. Cytokines and arachidonic metabolites produced during human immunodeficiency virus (HIV)-infected macrophage interactions: implications for the neuropathogenesis of HIV disease. J Exp Med. 1992; 176:1703–1718. [PubMed: 1460427]

Gray JA, Shi Y, Usui H, During MJ, Sakimura K, Nicoll RA. Distinct Modes of AMPA Receptor Suppression at Developing Synapses by GluN2A and GluN2B: Single-Cell NMDA Receptor Subunit Deletion In Vivo. Neuron. 2011; 71:1085–1101. [PubMed: 21943605]

Hofman FM, Dohadwala MM, Wright AD, Hinton DR, Walker SM. Exogenous tat protein activates central nervous system-derived endothelial cells. J Neuroimmunol. 1994; 54:19–28. [PubMed: 7523444]

Hudson L, Liu J, Nath A, Jones M, Raghavan R, Narayan O, Male D, Everall I. Detection of the human immunodeficiency virus regulatory protein tat in CNS tissues. J Neurovirol. 2000; 6:145–155. [PubMed: 10822328]

Hult B, Chana G, Masliah E, Everall I. Neurobiology of HIV. International review of psychiatry (Abingdon, England). 2008; 20:3–13.

Johnston PA, Sudhof TC. The multisubunit structure of synaptophysin. J Biol Chem. 1990; 265:8869–8873. [PubMed: 2111326]

Kaul M, Garden GA, Lipton SA. Pathways to neuronal injury and apoptosis in HIV-associated dementia. Nature. 2001; 410:988–994. [PubMed: 11309629]

Kaul M, Lipton SA. Mechanisms of Neuronal Injury and Death in HIV-1 Associated Dementia. Curr HIV Res. 2006; 4:307–318. [PubMed: 16842083]

Kim BO, Liu Y, Ruan Y, Xu ZC, Schantz L, He JJ. Neuropathologies in transgenic mice expressing human immunodeficiency virus type 1 Tat protein under the regulation of the astrocyte-specific glial fibrillary acidic protein promoter and doxycycline. Am J Pathol. 2003; 162:1693–1707. [PubMed: 12707054]

Kim HJ, Martemyanov KA, Thayer SA. Human Immunodeficiency Virus Protein Tat Induces Synapse Loss via a Reversible Process That Is Distinct from Cell Death. J Neurosci. 2008; 28:12604–12613. [PubMed: 19036954]

Kim HJ, Shin AH, Thayer SA. Activation of Cannabinoid Type 2 Receptors Inhibits HIV-1 Envelope Glycoprotein gp120-Induced Synapse Loss. Mol Pharmacol. 2011; 80:357–366. [PubMed: 21670103]

Kim HJ, Thayer SA. Lithium increases synapse formation between hippocampal neurons by depleting phosphoinositides. Mol Pharmacol. 2009; 75:1021–1030. [PubMed: 19188338]

Li W, Huang Y, Reid R, Steiner J, Malpica-Llanos T, Darden TA, Shankar SK, Mahadevan A, Satishchandra P, Nath A. NMDA Receptor Activation by HIV-Tat Protein Is Clade Dependent. J Neurosci. 2008; 28:12190–12198. [PubMed: 19020013]

Li W, Li G, Steiner J, Nath A. Role of Tat Protein in HIV Neuropathogenesis. Neurotox Res. 2009; 16:205–220. [PubMed: 19526283]

Liu L, Wong TP, Pozza MF, Lingenhoehl K, Wang Y, Sheng M, Auberson YP, Wang YT. Role of NMDA Receptor Subtypes in Governing the Direction of Hippocampal Synaptic Plasticity. Science. 2004; 304:1021–1024. [PubMed: 15143284]

NIH-PA Author Manuscript

NIH-PA Author Manuscript

NIH-PA Author Manuscript

Liu Y, Jones M, Hingtgen CM, Bu G, Laribee N, Tanzi RE, Moir RD, Nath A, He JJ. Uptake of HIV-1 tat protein mediated by low-density lipoprotein receptor-related protein disrupts the neuronal metabolic balance of the receptor ligands. Nat Med. 2000; 6:1380–1387. [PubMed: 11100124]

Liu Y, Wong TP, Aarts M, Rooyakkers A, Liu L, Lai TW, Wu DC, Lu J, Tymianski M, Craig AM, Wang YT. NMDA Receptor Subunits Have Differential Roles in Mediating Excitotoxic Neuronal Death Both In Vitro and In Vivo. J Neurosci. 2007; 27:2846–2857. [PubMed: 17360906]

Masliah E, Heaton RK, Marcotte TD, Ellis RJ, Wiley CA, Mallory M, Achim CL, McCutchan JA, Nelson JA, Atkinson JH, Grant I. Dendritic injury is a pathological substrate for human immunodeficiency virus-related cognitive disorders. HNRC Group. The HIV Neurobehavioral Research Center. Ann Neurol. 1997; 42:963–972. [PubMed: 9403489]

McMahon HT, Bolshakov VY, Janz R, Hammer RE, Siegelbaum SA, Sudof TC. Synaptophysin, a major synaptic vesicle protein, is not essential for neurotransmitter release. Proc Natl Acad Sci U S A. 1996; 93:4760–4764. [PubMed: 8643476]

Meyer G, Varoqueaux F, Neeb A, Oschlies M, Brose N. The complexity of PDZ domain-mediated interactions at glutamatergic synapses: a case study on neuroligin. Neuropharmacol. 2004; 47:724–733.

Midde N, Gomez A, Zhu J. HIV-1 Tat protein decreases dopamine transporter cell surface expression and vesicular monoamine transporter-2 function in rat striatal synaptosomes. J Neuroimmune Pharmacol. 2012; 7:629–639. [PubMed: 22570010]

Minagar A, Commins D, Alexander JS, Hoque R, Chiappelli F, Singer EJ, Nikbin B, Shapshak P. NeuroAIDS: Characteristics and Diagnosis of the Neurological Complications of AIDS. Molecular diagnosis & therapy. 2008; 12:25–43. [PubMed: 18288880]

Mishra A, Kim HJ, Shin AH, Thayer SA. Synapse Loss Induced by Interleukin-1β Requires Pre- and Post-synaptic Mechanisms. J Neuroimmune Pharmacol. 2012; 7:571–578. [PubMed: 22311599]

Perry S, Barbieri J, Tong N, Polesskaya O, Pudasaini S, Stout A, Lu R, Lu R, Kiebala M, Maggirwar S, Gelbard H. Human immunodeficiency virus-1 Tat activates calpain proteases via the ryanodine receptor to enhance surface dopamine transporter levels and increase transporter-specific uptake and Vmax. The Journal of Neuroscience. 2010; 30:14153–14164. [PubMed: 20962236]

Rehm H, Wiedenmann B, Betz H. Molecular characterization of synaptophysin, a major calcium-binding protein of the synaptic vesicle membrane. Embo J. 1986; 5:535–541. [PubMed: 3086086]

Sa MJ, Madeira MD, Ruela C, Volk B, Mota-Miranda A, Paula-Barbosa MM. Dendritic changes in the hippocampal formation of AIDS patients: a quantitative Golgi study. Acta Neuropathol (Berl). 2004; 107:97–110. [PubMed: 14605830]

Scheiffele P, Fan J, Choih J, Fetter R, Serafini T. Neuroligin expressed in nonneuronal cells triggers presynaptic development in contacting axons. Cell. 2000; 101:657–669. [PubMed: 10892652]

Shen M, Thayer SA. The cannabinoid agonist Win55,212–2 inhibits calcium channels by receptor-mediated and direct pathways in cultured rat hippocampal neurons. Brain Res. 1998; 783:77–84. [PubMed: 9479052]

Shin AH, Kim HJ, Thayer SA. Subtype selective NMDA receptor antagonists induce recovery of synapses lost following exposure to HIV-1 Tat. Br J Pharmacol. 2012; 166:1002–1017. [PubMed: 22142193]

Speth C, Stockl G, Mohsenipour I, Wurzner R, Stoiber H, Lass-Florl C, Dierich MP. Human immunodeficiency virus type 1 induces expression of complement factors in human astrocytes. J Virol. 2001; 75:2604–2615. [PubMed: 11222683]

Theodore S, Cass W, Dwoskin L, Maragos W. HIV-1 protein Tat inhibits vesicular monoamine transporter-2 activity in rat striatum. Synapse. 2012; 66:755–757. [PubMed: 22517264]

Togashi H, Abe K, Mizoguchi A, Takaoka K, Chisaka O, Masatoshi T. Cadherin Regulates Dendritic Spine Morphogenesis. Neuron. 2002; 35:77–89. [PubMed: 12123610]

tom Dieck S, Sanmarti-Vila L, Langnaese K, Richter K, Kindler S, Soyke A, Wex H, Smalla KH, Kampf U, Franzer JT, Stumm M, Garner CC, Gundelfinger ED. Bassoon, a Novel Zinc-finger CAG/Glutamine-repeat Protein Selectively Localized at the Active Zone of Presynaptic Nerve Terminals. J Cell Biol. 1998; 142:499–509. [PubMed: 9679147]

Tozzi V, Balestra P, Lorenzini P, Bellagamba R, Galgani S, Corpolongo A, Vlassi C, Larussa D, Zaccarelli M, Noto P, Visco-Comandini U, Giulianelli M, Ippolito G, Antinori A, Narciso P.

NIH-PA Author Manuscript

NIH-PA Author Manuscript

NIH-PA Author Manuscript

Prevalence and risk factors for human immunodeficiency virus–associated neurocognitive impairment, 1996 to 2002: Results from an urban observational cohort. J Neurovirol. 2005; 11:265–273. [PubMed: 16036806]

Waataja JJ, Kim HJ, Roloff AM, Thayer SA. Excitotoxic loss of post-synaptic sites is distinct temporally and mechanistically from neuronal death. J Neurochem. 2008; 104:364–375. [PubMed: 17944868]

Westendorp MO, Frank R, Ochsenbauer C, Stricker K, Dhein J, Walczak H, Debatin KM, Krammer PH. Sensitization of T cells to CD95-mediated apoptosis by HIV-1 Tat and gp120. Nature. 1995; 375:497–500. [PubMed: 7539892]

Wiedenmann B, Franke W. Identification and localization of synaptophysin, an integral membrane glycoprotein of Mr 38,000 characteristic of presynaptic vesicles. Cell. 1985; 41:1017–1028. [PubMed: 3924408]

Wiley CA, Baldwin M, Achim CL. Expression of regulatory and structural mRNA in the central nervous system. AIDS. 1996; 10:943–947.

Wiley CA, Masliah E, Achim CL. Measurement of CNS HIV burden and its association with neurologic damage. Adv Neuroimmunol. 1999; 4:319–325. [PubMed: 7874400]

Xiao H, Neuveut C, Lee H, Benkirane M, Rich EA, Murphy PM, Jeang KT. Selective CXCR4 antagonism by Tat: implications for in vivo expansion of coreceptor use by HIV-1. Proc Natl Acad Sci U S A. 2000; 97:11466–11471. [PubMed: 11027346]

Ziv NE. Recruitment of Synaptic Molecules during Synaptogenesis. The Neuroscientist. 2001; 7:365–370. [PubMed: 11597095]

Ziv NE, Garner CC. Cellular and molecular mechanisms of presynaptic assembly. Nat Rev Neurosci. 2004; 5:385–399. [PubMed: 15100721]

NIH-PA Author Manuscript
NIH-PA Author Manuscript
NIH-PA Author Manuscript

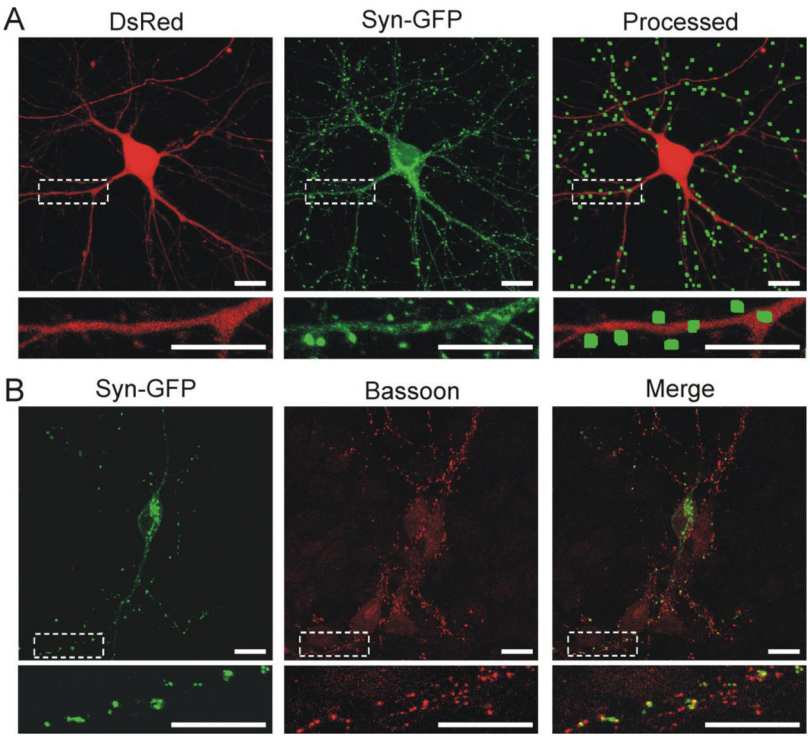

Figure 1. Synaptophysin-GFP puncta represent presynaptic terminals

A, representative confocal images were collected and processed as described in Methods. Maximum z-projections show a neuron expressing DsRed2 (DsRed) and Syn-GFP. Syn-GFP puncta were identified from compressed z-stacks of confocal images by filtering for puncta size and fluorescence intensity. Puncta were dilated and overlaid on the DsRed maximum projection (Processed). Heavy intracellular labeling in the soma was not counted by the algorithm. Insets are enlarged images of the boxed regions. Scale bars represent 10 μm. B, representative confocal images of neurons expressing Syn-GFP and immunolabeled for Bassoon. Syn-GFP puncta co-localized with Bassoon immunoreactivity (Merge). Note that non-transfected cells were also present in the field, and thus not all Bassoon-immunoreactive puncta (red) co-localize (yellow) with a Syn-GFP puncta (green). Insets are enlarged images of the boxed regions. Scale bars represent 10 μm.

NIH-PA Author Manuscript
NIH-PA Author Manuscript
NIH-PA Author Manuscript

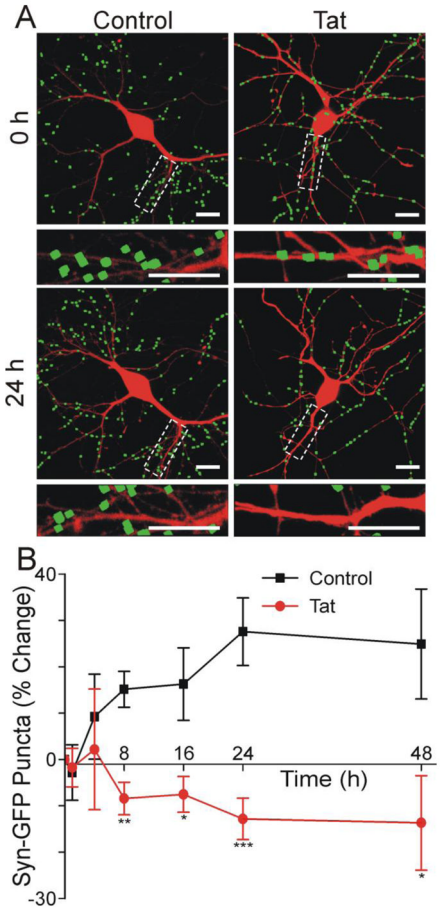

Figure 2. HIV-1 Tat induces loss of presynaptic terminals

A, representative processed images show neurons before (0 h) and after (24 h) no treatment (Control) or treatment with 50 ng/mL Tat (Tat). Insets are enlarged images of the boxed regions. Scale bars represent 10 μm. B, Graph shows % change in number of Syn-GFP puncta over a 48 h interval ($n \geq 6$ for each time point). Neurons were either untreated (Control, black squares) or treated with 50 ng/mL Tat (Tat, red circles) after the initial time point (t = 0 h). *, $p<0.05$, **, $p<0.01$, ***, $p<0.001$ vs. Control values at corresponding time point (ANOVA with Tukey's post-test). All data are expressed as mean ± SEM.

NIH-PA Author Manuscript

NIH-PA Author Manuscript

NIH-PA Author Manuscript

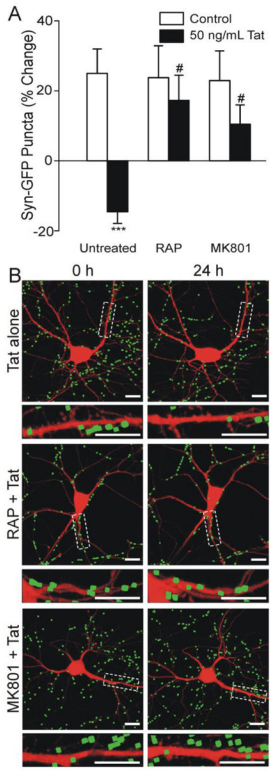

Figure 3. Tat-induced Syn-GFP loss requires postsynaptic activity

A, Bar graph summarizes % change in number of Syn-GFP puncta over 24 h under control conditions (open bars) or in the presence of 50 ng/mL Tat (solid bars) ($n \geq 9$ for all groups). Neurons were imaged in the absence (Untreated) or the presence of 50 nM RAP or 10 μM MK801 as indicated. ***, $p < 0.001$ vs. Control; #, $p<0.05$ vs. Tat alone (ANOVA with Tukey's post-test). All data are expressed as mean ± SEM. B, representative processed images of neurons before (0 h) or after (24 h) treatment with 50 ng/mL Tat. Neurons were either untreated (Tat alone), or pretreated with 50 nM RAP (RAP + Tat) or 10 μM MK801 (MK801 + Tat). Insets are enlarged images of the boxed regions. Scale bars represent 10 μm.

NIH-PA Author Manuscript
NIH-PA Author Manuscript
NIH-PA Author Manuscript

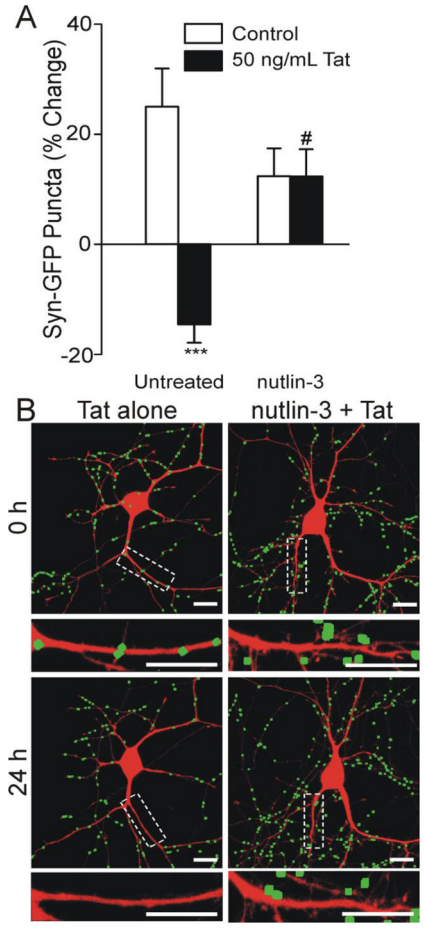

Figure 4. Tat-induced Syn-GFP loss requires E3 ligase activity

A, Bar graph summarizes % change in number of Syn-GFP puncta over 24 h under control conditions (open bars) or in the presence of 50 ng/mL Tat (solid bars) ($n \geq 9$ for all groups). Neurons were imaged in the absence (Untreated) or the presence of 1 μM nutlin-3. ***, $p < 0.001$ vs. Control; #, $p<0.05$ vs. Tat (ANOVA with Tukey's post-test). All data are expressed as mean ± SEM. B, representative processed images of neurons before (0 h) or after (24 h) treatment with 50 ng/mL Tat. Neurons were either untreated (Tat alone), or pretreated with 1 μM nutlin-3 (Nutlin-3 + Tat). Insets are enlarged images of the boxed regions. Scale bars represent 10 μm.

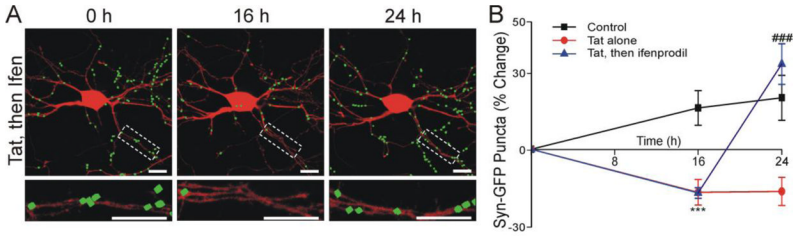

Figure 5. Tat-induced Syn-GFP loss is reversible

A, representative processed images of a neuron before (0h) and 16 h or 24 h after treatment with 50 ng/mL Tat. 10 μM ifenprodil was applied immediately after acquisition of the image at t = 16 h. Tat was present throughout the experiment. Insets are enlarged images of the boxed regions. Scale bars represent 10 μm. B, Graph summarizes % changes in number of Syn-GFP puncta in the absence (Control), or presence of 50 ng/mL Tat ($n \geq 6$ for all groups). After 16 h exposure to Tat, neurons were then left untreated (Tat alone) or treated with 10 μM ifenprodil (Tat, then ifenprodil). All data are expressed as mean ± SEM. ***, $p < 0.001$ vs. Control at 16 h, ###, $p < 0.001$ vs. Tat alone at 24 h (ANOVA with Tukey's post-test).

NIH-PA Author Manuscript
NIH-PA Author Manuscript
NIH-PA Author Manuscript